COPY NO. 62

Report MDC E0056
15 December 1969

A TWO-STAGE FIXED WING SPACE TRANSPORTATION SYSTEM

FINAL REPORT

Volume I Condensed Summary

Contract No. NAS 9-9204 Schedule II

MCDONNELL DOUGLAS CORPORATION

FOREWORD

This report in three volumes, summarizes the results for a McDonnell Douglas Phase A study of a Two Stage-Fixed Wing Space Transportation System for NASA MSC, and is submitted in accordance with NASA Contract NAS9-9204 Schedule II. The three volumes of the report are: Volume I - Condensed Summary; Volume II - Preliminary Design; Volume III - Mass Properties. This is Volume I which presents a condensed summary of our study results.

This was a five month study commencing 16 July 1969 with the final report submitted on 15 December 1969. The objectives of the study were to provide verification of the feasibility and effectiveness of the MSC in-house studies and provide design improvements, to increase the depth of engineering analyses and to define a development approach. The preliminary design was to be accomplished in accordance with the design requirements specified in the statement of work, and with more detailed requirements provided by MSC at the outset of the study.

After the study had progressed to about the mid-point, NASA redirected the study from a baseline 12,500 lbs payload orbiter to a 25,000 lbs payload orbiter and changed the payload compartment size from 11 ft diameter by 44 ft, long to a 15 ft diameter by 60 ft long. Directly after this change the program was interrupted so that MDAC could respond to special emphasis requirements imposed by the September Space Shuttle Management Council Meeting.

In the interest of clarity and expediting the report, the additional configurations studied will not be covered in the document. Only the configuration having a 25,000 lbs payload in a 15 ft diameter by 60 ft long payload compartment is described in this report. However the information on other configurations had been transmitted previously to NASA as the work progressed.

The study included eight tasks: Flight Dynamics Analysis, Thermal Protection System, Subsystem Analyses, Design; Mass Properties Analysis; Mission Analysis; Design Sensitivity Analyses; and Programmatic Analyses.

The study was managed and supervised by Winston D. Nold, Study Manager of McDonnell Douglas Astronautics Company - Eastern Division. NASA technical direction was administered through James A. Chamberlin, and contractual direction was provided by Willie S. Beckham from NASA Manned Spacecraft Center.

TABLE OF CONTENTS

LIST OF EFFECTIVE PAGES

i through ii
1 through 18

1. Summary - The growth of future manned space expoloration is dependent upon the development of a reusable space transportation system with operational practices similar to present day aircraft procedures. Such a system could achieve a dramatic reduction of operational costs and allow a rapid expansion of space flight.

A two stage configuration satisfying these requirements has been conceived by NASA-MSC. An important feature of this configuration is that both the orbiter and booster have fixed wings and tail and look similar to conventional aircraft. The fixed wing provides good subsonic cruise and horizontal landing characteristics which are very similar to present day high performance aircraft.

The ability to enter the atmosphere with a fixed wing is made possible by configuring the vehicle to be aerodynamically stable at high angles of attack of approximately 60°. This effectively exposes only the bottom surface to the entry heating, which in turn is also considerably reduced because of the low planform loading. Sufficient analysis has been accomplished to show that this concept is feasible. A vehicle can be aerodynamically configured to have a hypersonic through subsonic velocity high α trim point and also be able to fly subsonically at a trim low α.

A reaction control system is used to provide on-orbit attitude control and terminal rendezvous and docking translation ΔV. The RCS also provides attitude damping and roll attitude control for lift vector orientation about the velocity vector during entry.

Designs of both stages incorporate conventional structural design techniques. The fixed wing is of conventional construction, except for the heat protection. The fuselage uses an integral tank structure with associated frames to pick up the concentrated loads. The fan cruise engines are fixed in the forward fuselage which aids in balancing the vehicle and simplifies the installation. The primary heat protection is provided by silica cloth faced hardened insulation and pyrolized carbon laminate composite.

We have concluded that this concept is a viable configuration. The technical analysis and design results bear this out. As appropriate, pertinent analyses and data generated by the NASA-MSC in-house study is included in the report.

2. Design Characteristics - The reusable space shuttle described in this report is a two stage fixed wing system. Both stages - booster and orbiter - have a similar shape. The booster is powered by ten (10) high pressure bell engines of 400,000 lbs. sea level thrust. The orbiter has two (2) similar engines. The system is sized to carry a 25,000 lbs. payload to a 270 NM 55° inclination orbit. Both vehicles are capable of low level horizontal flight with forward fuselage mounted turbofan engines. Figure 1 shows a three view of the configuration and presents some of the pertinent characteristic data. Figures 2 and 3 present a summary of the weight breakdown and mission history weight for the orbiter and booster.

VEHICLE CHARACTERISTICS

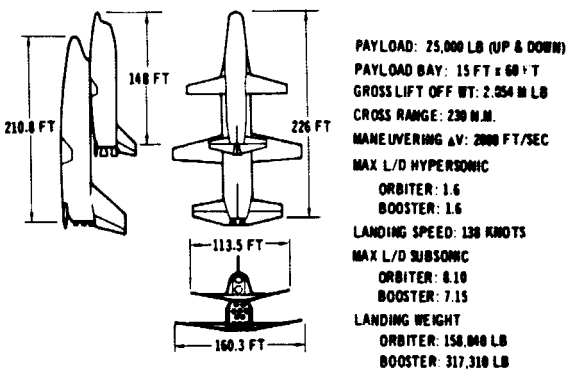

Figure 1

WEIGHT SUMMARY - 25K PAYLOAD

GROUP	ORBITER	BOOSTER
BODY STRUCTURE	39.180	92.700
WING	14.700	37.410
TAIL	6.740	16.640
THERMAL PROTECTION	18.450	30.130
LANDING GEAR & DRAG CHUTE	6.400	12.750
MAIN PROPULSION SYSTEM	16.600	75.885
AIR BREATHING ENGINES & SYSTEM	14.700	30.510
RCS & TANKS	2.500	3.500
AERODYNAMIC CONTROLS	2.700	4.650
HYDRAULIC SYSTEM	1.590	2.930
ELECTRICAL POWER SYSTEM	3.280	3.000
G&N, INSTRUMENTATION, COMMUNICATIONS, CREW STATION & CONTROLS, & ECS	4.260	2.605
RESIDUALS	1.540	3.400
RESERVE	600	1.200
CREW & EQUIPMENT	600	0
CONTINGENCY	0	0
LANDED WEIGHT - POUNDS	133.840	317.310

Figure 2

WEIGHT SUMMARY - 25K PAYLOAD

CONFIGURATION	ORBITER	BOOSTER
LANDED WEIGHT LESS PAYLOAD	133.840	
PAYLOAD	25.000	
LANDED WEIGHT	158.840	317.310
FLY-HOME PROPELLANTS	3.070	80.000
FLUID LOSSES	11.910	17.420
ON-ORBIT MANEUVER (ΔV - 2000 FPS)	28.460	
ORBIT INJECTION WEIGHT	202.280	
INJECTION PROPELLANT (ΔV-15.965 FPS)	400.000	
SEPARATION WEIGHT	602.280	414.730
BOOST PROPELLANTS (ΔV - 14.635 FPS)		1.837.180
STAGE LIFT-OFF WEIGHT	602.280	2.251.910
TOTAL LIFT-OFF WEIGHT - POUNDS	2.854.190	

Figure 3

2.1 Orbiter - The orbiter accommodates a crew of two and has a payload capability of 25,000 lbs. to and from orbit. The payload bay is 15 ft. in diameter and 60 ft. long. The inboard profile and geometric data is shown in Figure 4 and 5.

Conventional airplane controls are employed for subsonic cruise and landing. A retractable tricycle landing gear is provided. The wing has double slotted flaps which allows landing speeds under 140 knots on a standard runway. Four (4) turbofan engines provide the power during this phase of flight.

INBOARD PROFILE - ORBITER

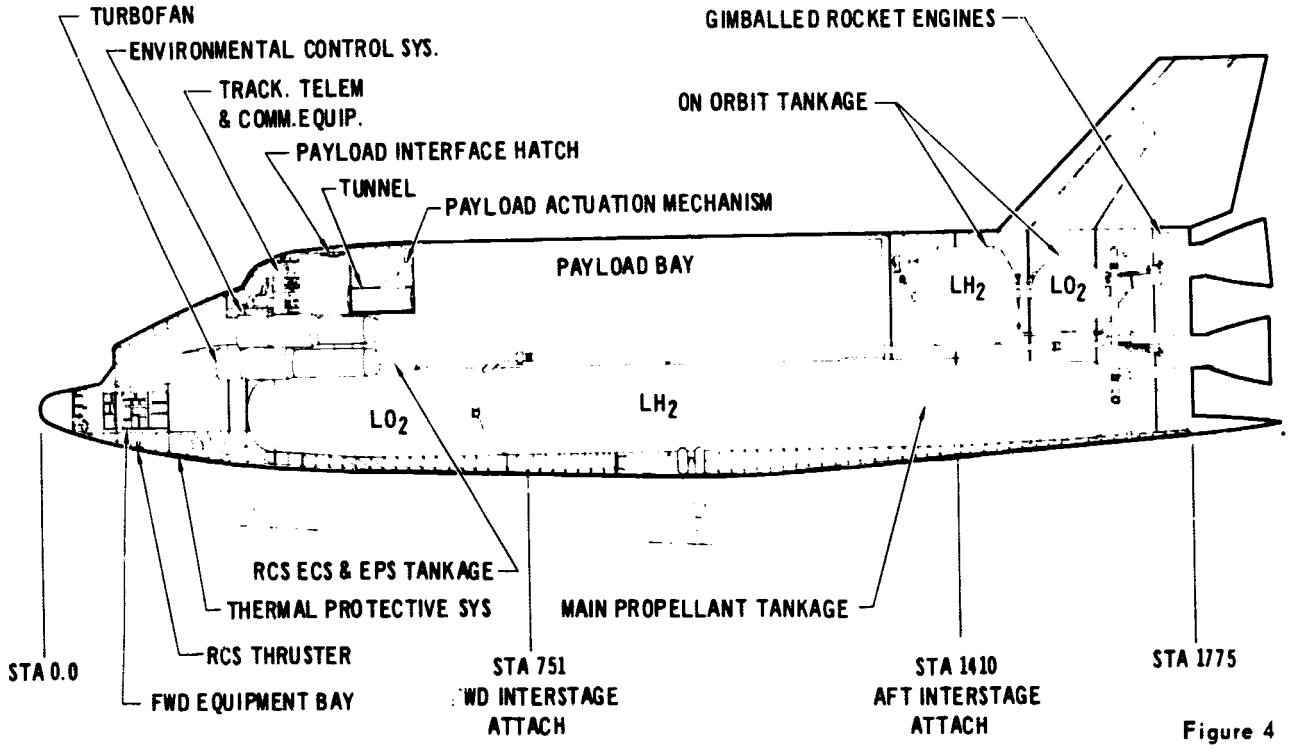

Figure 4

GEOMETRIC DATA - ORBITER

Vehicle Weights		**Horizontal Tail Geometry**	
Gross Weight	602,280 lb.	Wetted Area	1,554 ft²
Entry Weight	1[illegible],910 lb.	Theoretical Area	903 ft²
Landing Weight	158,840 lb.	Exposed Area	777 ft²
		Span (b)	65 ft
Vehicle Geometry		Aspect Ratio (AR)	4.68:1
Total Projected		L. E. Sweep	10°
Planform Area	5,[illegible]30 ft	Taper Ratio	.354:1
		Root Chord (C_R)	20.5 ft
Body Geometry		Tip Chord (C_T)	7.25 ft
Wetted Area	11,967 ft²	M.A.C. ($\bar{C}$)	14.9 ft
ML Volume	66,480 ft³	Airfoil Section	NACA 0012-64
Length	148 ft	Elevator	56% C X b
Bottom Wetted Area	3,027 ft²	Elevator Deflection	± 40°
Wing Geometry		**Vertical Tail Geometry**	
Wetted Area	2,692 ft²	Wetted Area	910 ft²
Theoretical Area	1,850 ft²	Theoretical Area	455 ft²
Exposed Area	1,346 ft²	Exposed Area	455 ft²
Span (b)	113.5 ft	Span (b)	21.2 ft
Aspect Ratio (AR)	7:1	Aspect Ratio (AR)	.98:1
Dihedral Angle	7°	L. E. Sweep	45°
L. E. Sweep	14°	Taper Ratio	.472:1
Taper Ratio	.353:1	Root Chord (C_R)	29.2 ft
M.A.C. ($\bar{C}$)	17.5 ft	Tip Chord (C_T)	13.75 ft
Root Chord (C_R)	24.1 ft	M.A.C. ($\bar{C}$)	22.4 ft
Tip Chord (C_T)	8.5 ft	Airfoil Section	NACA 0012-64
Airfoil Section at Root (body ℄)	NACA 0014-64	Rudder	30% C X b
Airfoil Section at Tip	NACA 0010-64	Rudder Deflection	± 25°
Flaps, Double Slotted	30% C X 60% b exposed		
Flaps Movement Max	55°		
Ailerons	25% C X 30% b exposed		
Ailerons Deflection	± 20°		

Figure 5

Two (2) bell nozzle high pressure boost engines using LO_2 and LH_2 propellants provide power for initial orbit injection. These same engines used in a pressure fed mode and drawing propellant from separate tanks, provide the power for on-orbit translation and deorbit.

The structural design approach uses the main propellant tanks as an integral part of the fuselage structure. The tanks are aluminum and formed into a double bubble design with a central web. Titanium longerons, frames and skin make up the rest of the fuselage structure. The wings, stabilizer, and vertical fin use a titanium integral stiffened skin spar and rib construction.

The thermal protection consists of hardened compacted fibers on the fuselage bottom and sides, and the under side of the wing and stabilizer. Pyrolized carbon laminates are used for the fuselage nose and the leading edges of the wing, stabilizer and vertical fin.

Other key features shown on the inboard profile are: (1) the forward location of the turbofan cruise engines to provide a favorable CG, (2) on-orbit propellant located aft near the main rocket engines to minimize trapped fluid and line losses, (3) the forward interstage attach point is located at the orbiter gross weight CG so that stage separation is primarily translation with a minimum of rotation, and (4) the electrical power equipment, batteries and fuel cells are located in the forward section to aid in providing a favorable CG.

2.2 Booster - The booster is similar in shape to the orbiter with a fixed wing and conventional aerodynamic controls for horizontal flight. The booster has the capability for both manned and unmanned operations. Figures 6 and 7 show an inboard profile and present some of the geometric data.

The booster is powered during ascent by ten (10) bell nozzle 400,000 lbs. thrust rocket engines using LO_2 and LH_2 propellants. Six (6) turbofan cruise engines, installed well forward to aid in CG control are provided for flying back to the launch site giving an all azimuth launch capability. The structural design of the booster is similar to the orbiter but somewhat simpler because no payload bay discontinuity is present.

The thermal protection consists of only hardened compacted fibers over the high temperature regions of the fuselage and aerodynamic surfaces.

3. Structural Design - The primary structural design of the orbiter is illustrated in Figure 8. Basic body bending/shear structure is made up of upper longerons adjacent to the payload compartment and the propellant tank structures below the payload joined by fuselage side skin panels. Two integrally stiffened cylindrical tank shells are joint at a common keel web in a "double bubble" arrangement. Side panels are single skin, stiffened by corrugations. These panels and payload doors are the upper surface of

INBOARD PROFILE - BOOSTER

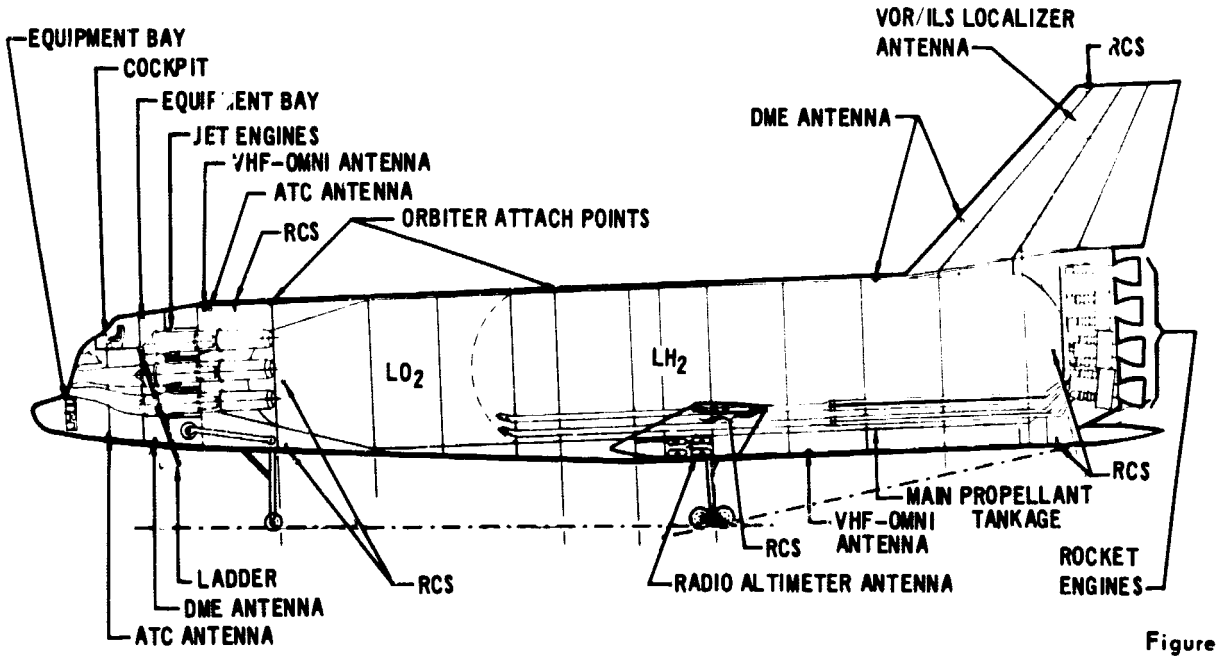

Figure 6

GEOMETRIC DATA - BOOSTER

Vehicle Weights		**Horizontal Tail Geometry**	
Gross Weight	2,251,910 lb.	Wetted Area	3,216 ft^2
Entry Weight	414,730 lb.	Theoretical Area	2,152 ft^2
Landing Weight	317,310 lb.	Exposed Area	1,608 ft^2
		Span (b)	101.6 ft
Vehicle Geometry		Aspect Ratio (AR)	4.8:1
Total Projected Planform Area	10,152 ft^2	L. E. Sweep	10°
		Taper Ratio	.397:1
Body Geometry		Root Chord (C_R)	28.6 ft
Wetted Area	21,800 ft^2	Tip Chord (C_T)	11.34 ft
Mf. Volume	164,380 ft^3	M.A.C. ($\bar{C}$)	22.5 ft
Length	211 ft	Airfoil Section	NACA 0012-64
Bottom Wetted Area	5,840 ft^2	Elevator	56% C X b
		Elevator Deflection	± 40°
Wing Geometry		**Vertical Tail Geometry**	
Wetted Area	5,408 ft^2	Wetted Area	2,094 ft^2
Theoretical Area	3,700 ft^2	Theoretical Area	1,047 ft^2
Exposed Area	2,704 ft^2	Exposed Area	1,047 ft^2
Span (b)	160 ft	Span (b)	30 ft
Aspect Ratio (AR)	6.92:1	Aspect Ratio (AR)	.9:1
Dihedral Angle	7°	L. E. Sweep	45°
L. E. Sweep	14°	Taper Ratio	.462:1
Taper Ratio	.353:1	Root Chord (C_R)	43.3 ft
M.A.C. ($\bar{C}$)	24.8 ft	Tip Chord (C_T)	20 ft
Root Chord (C_R)	34 ft	M.A.C. ($\bar{C}$)	32.7 ft
Tip Chord (C_T)	12 ft	Airfoil Section	NACA 0012-64
Airfoil Section at Root (body ℄)	NACA 0014-64	Rudder	30% C X b
Airfoil Section at Tip	NACA 0010-64	Rudder Deflection	± 25°
Flaps, Double Slotted	30% C X 60% b exposed		
Flaps Movement Max	55°		
Ailerons	25% C X 30% b exposed		
Ailerons Deflection	± 20°		

Figure 7

the fuselage. Tank shell structure is aluminum for compatibility with propellants and protected by moldline Thermal Protection System (TPS) shingles. Shell stiffening frames spaced at 20 inch intervals also support the TPS, upper side panels and longerons. Frames are titanium to minimize heat conductance to the tanks. The upper structures are warm during launch and entry, and, also are titanium for good strength/weight ratio at elevated temperatures.

The forward fuselage structural shell is titanium single skin stiffened by corrugations and frames, and forms the M.L. except where non-structural surfaces exist, such as engine and nose landing gear doors. Intercostals and frames are transition structures between the forward fuselage and the propellant tank.

The hardened compacted fiber is bonded directly to the forward fuselage shell surface aft to the propellant tanks. In the main area twenty inch long HCF shingle panels form the bottom and the sides up to approximately six feet above the chine lines. Single thickness beaded titanium panels form the surface between the HCF shingles and fuselage structural side skins. HCF is bonded to fiberglass honeycomb

panels which distribute surface pressure loads to small lateral shingle support beams. The beams are attached to the tank shell stiffening frames by titanium links spaced at approximately 24 inches across the fuselage. Removeable Pi shaped elements attached to the beams retain the shingles and provide a gap for thermal expansion.

The two orbiter boost engines are supported by a tripod arrangement of linkage thrust structures for each engine. Linkage loads are transferred to the keel web, upper longerons and frames at stations 1635 and 1717. The frames also serve as main support elements for vertical and horizontal tails.

Turbofan engines are supported on longitudinal intercostals attached to the forward fuselage shell and by bulkheads at stations 320, 362 and 400. The bulkheads also serve as primary structures supporting cabin pressurization and nose gear loads.

The orbiter wing is attached to the fuselage at three major frames in the plane of wing spars at stations 391, 972 and 1024, and to the keel web in the plane of the wing ℄ rib. Normal wing loads and symmetrical wing torque are supported at the frames and drag loads are supported at the keel web.

The primary two cell wing box is made of 6Al-4V titanium with integrally stiffened skins of conventional arrangement, Figure 9. The main box is protected from reentry heating by external insulation (HCF) bonded to the lower surface. The thickness of the HCF is established to not exceed a bond line temperature of 500°F. The upper wing surface experiences temperatures of less than 800°F, and, therefore, is not insulated. The orbiter wing leading edge is constructed of carbon/

STRUCTURAL ARRANGEMENT - ORBITER

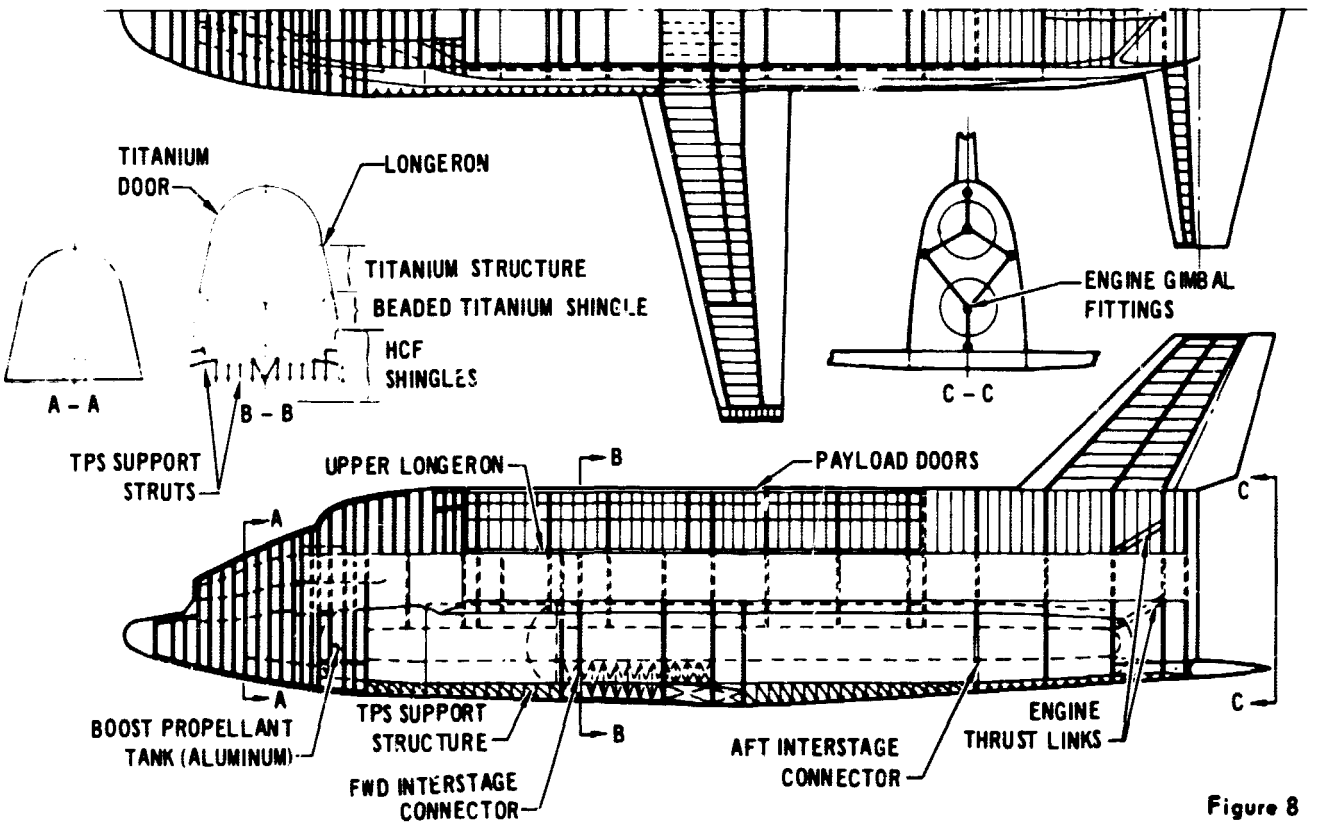

Figure 8

carbon composite honeycomb sandwich material that serves as structure and requires no additional TPS. The lower side of the wing leading edge in the inboard region is the area of the most severe heating. In this area the carbon/carbon composite will exhibit an oxidation erosion with each entry. To keep from having an excessive thickness and ending up with a distorted airfoil, a replaceable slipper leading edge is proposed as shown in Figure 10. The slipper thickness is sized to allow about 10 entries, and then can be easily replaced. The titanium structural box is insulated from L.E. radiative heat by a layer of HCF on the front spar.

The booster fuselage is similar in concept to the orbiter fuselage. The main propellant tanks are "integral" aluminum body structure and carry overall vehicle loads, as well as, internal pressures. The forward fuselage primary structure is the outer shell which consists of stiffened titanium skins and frames, protected from ascent and reentry heating with external HCF similar to the arrangement on the orbiter forward fuselage. The booster wing leading edge experiences lower temperatures, relatively, and is a titanium structure with external insulation (HCF).

WING STRUCTURAL ARRANGEMENT - ORBITER

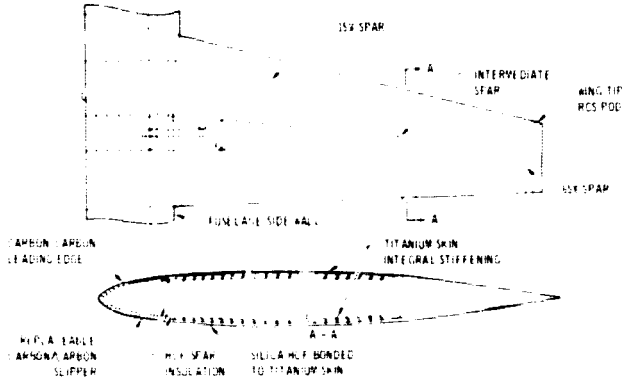

Figure 9

REPLACEABLE "SLIPPER" LEADING EDGE CONSTRUCTION
Slipper Designed for 10 Flights -

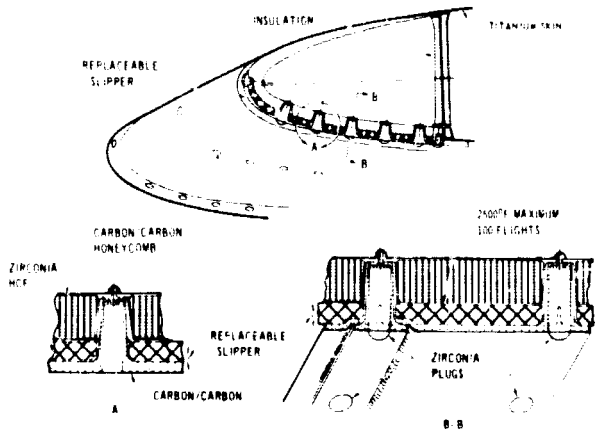

Figure 10

4. Aerodynamics and Performance

4.1 Aerodynamics - Aerodynamic analyses have been performed for each of the various flight regimes from liftoff to landing for the nominal mission. Mission considerations have resulted in the establishment of several aerodynamic configuration requirements: (1) high angle of attack (α = 60°) trim capability throughout the hypersonic/supersonic portion of entry with controls fixed; (2) static stability in pitch and yaw with neutral stability in roll; (3) the capability to trim subsonically at both high (60°) and low (5°) angles of attack with adequate transitional control; (4) handling qualities for subsonic cruise, approach and landing typical of present high performance aircraft. These requirements, in turn, have led to configuration selection guidelines which can be summarized for entry as: (1) the lower surfaces of the body-wing-tail combination should be smooth and continuous to minimize flow interaction; (2) pitch trim will be obtained by cambering the flat fuselage bottom fore and aft of the center of gravity in combination with the horizontal tail; (3) lateral stability will be obtained by wing dihedral (7°);

(4) directional stability obtained by differential fuselage side wall angles for and aft of the center of gravity (i.e., 5° cant angle on the forward section and straint sidewalls aft such that at small angles of sideslip flow impingement will produce stabilizing moments); (5) reaction control system for stability augmentation; (6) low W/SC_L ($\sim$ 50 psf). Similar guidelines were established for the subsonic cruise, approach and land portion of the flight: (1) fixed wing design with low sweep (14° leading edge), high aspect ratio (AR = 7) with conventional ailerons and double-slotted flaps for landing; (2) conventional vertical/horizontal tail, rudder/elevator; (3) sufficient turbofan power and L/D for typical airplane handling qualities during approach and landing. Consideration of these requirements/guidelines, and various parametric studies have led to the selected configuration. Prime emphasis has been placed on the orbiter, however, similarity between the orbiter and booster results in most of the aerodynamic characteristics being common.

The launch configuration results presented in Figure 11 have been developed using the low speed wind tunnel data obtained from Langley Research Center. These data must be considered as preliminary estimates. The drag is adequate for preliminary launch trajectory calculations. In addition, the negative Cm_α and positive Cm_β indicate an inherent stability exists.

LAUNCH CONFIGURATION AERODYNAMIC CHARACTERISTICS

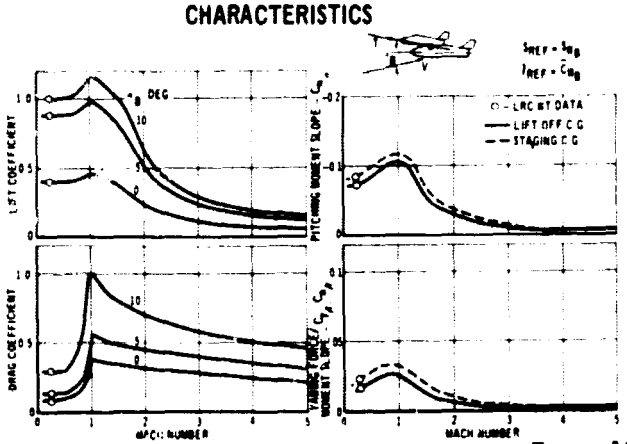

Figure 11

The Hypersonic Arbitrary-Body Aerodynamic Computer Program was utilized to predict the hypersonic aerodynamics for the orbiter and booster configurations. The results of this analysis of the orbiter as presented in Figure 12, show that the orbiter can be trimmed in the region of $C_{L\,max}$ (50° to 60° angle of attack) with a center-of-gravity (c.g.) location between 53% to 59% of the fuselage length. The forward c.g. limit is the point at which the vehicle would trim without an elevator, whereas the aft limit is a stability boundary beyond which no stable trim point exists. For a down elevator (positive deflection) of approximately 25° there are no stable trim points. Also shown is the trim lift coefficient (C_L) and lift-to-drag ratio (L/D). The respective maximum values are 1.85 and 1.6 at angles of attack of 52° and 20°. At the proposed entry angle of attack of 60°, C_L = 1.8 and L/D = .5.

An estimation of the hypersonic static and dynamic derivatives was also made. The data indicate the vehicle is dynamically stable in yaw, pitch, and roll; however, the vehicle is statically unstable in yaw for angles of attack less than 55 degrees.

ORBITER HYPERSONIC AERO CHARACTERISTICS

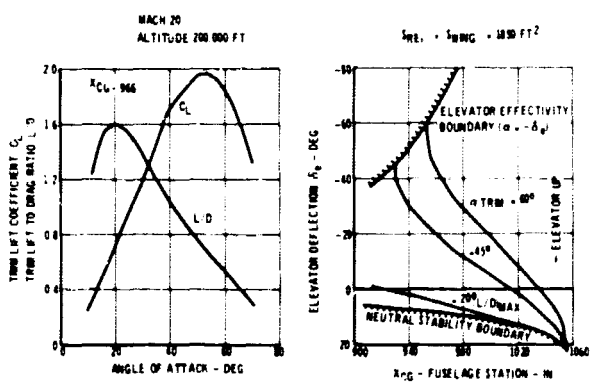

Figure 12

Subsonic aerodynamic characteristics for the orbiter configuration have been derived from a NASA Langley wind tunnel test. These test data were modified to reflect small configuration variations

including nose fineness ratio, tail size, and horizontal tail aspect ratio changes. Modifications were also made to the basic data in the angle of attack range between 45° and 75° to account for the difference between the subcritical test conditions and the super-critical flight Reynolds numbers. The resulting orbiter stability is shown in Figure 13 for two center of gravity locations and including effects of elevator deflection. Two separate angle of attack regions exist for stable trim ($-Cm_\alpha$). Reentry attitudes lie in the high angle of attack trim region and adequate elevator control power exists to break this trim point and to perform the subsonic transition to the low angle of attack trim region for a center of gravity position between 52% and 57% of body length.

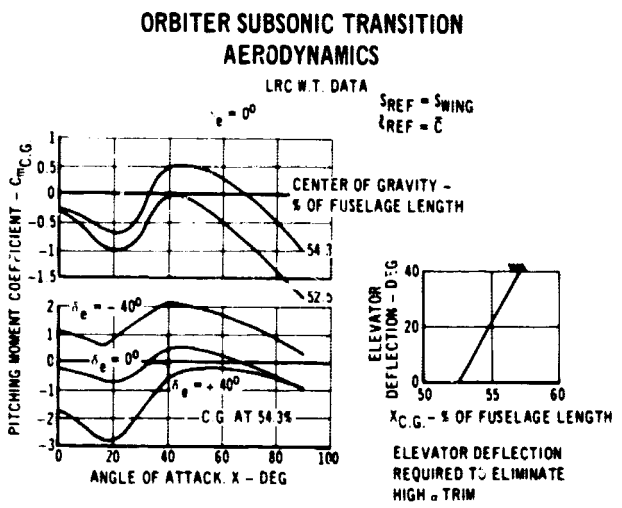

Figure 13

The estimated orbiter low angle of attack trim lift coefficient and lift to drag ratio for the subsonic flight Reynolds number is shown in Figure 14. The cruise configuration data (flap deflection, $S_F = 0$) is based on wind tunnel data previously discussed. The maximum lift coefficient is somewhat less than modern airliners primarily because the standard NACA symmetrical airfoil used on the orbiter and booster (selected to alleviate transonic loading during ascent) does not exhibit a high $C_{L_{max}}$. The maximum lift to drag ratio is also less than a typical transport aircraft because of the higher drag associated with the base area and fuselage wetted area. The design 30% chord double-slotted flaps covering 60% of the exposed span yield landing speeds ($1.1\ V_{stall}$) less than 140 kts and produce good horizontal take-off characteristics, high C_L and moderately high L/D. Figure 14 also shows the estimated flap effects for landing ($\delta_F = 55°$) and take-off ($\delta_F = 20°$). The techniques used in obtaining these estimations yield good agreement with DC-8-61 flight test data and DC-10 wind tunnel data.

Due to the similarity of the orbiter and booster, the booster trim lift coefficients are nearly identical to those of the orbiter. However, the large base area of the booster results in a cruise configuration $(L/D)_{max}$ of 7.2 compared to 8.1 for the orbiter.

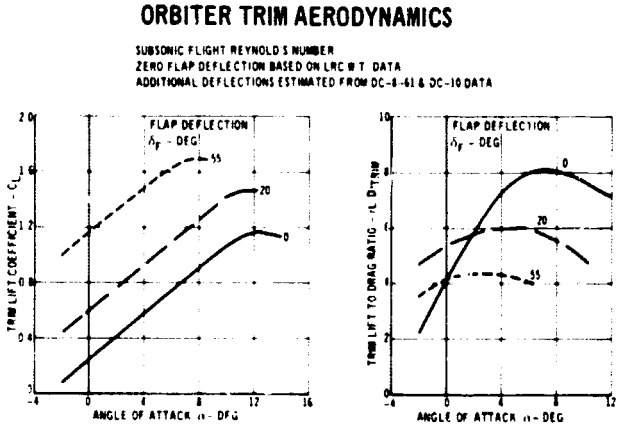

Figure 14

4.2 Performance - A point-mass launch optimization computer program was used to compute an ascent trajectory to a 55° inclination, 51-100 NM orbit. The significant parameters are presented in Figure 15. Note that maximum dynamic pressure is about 500 PSF, and that the engines were throttled to keep from exceeding 2.5 g's during 1st stage, and 3 g's during 2nd stage. The earth reference insertion velocity was 24,965 ft. per second. The velocity losses due to gravity, drag, back pressure and maneuvering totaled 5527 ft. per second and giving a nominal ideal velocity requirement of 30,492 ft. per second.

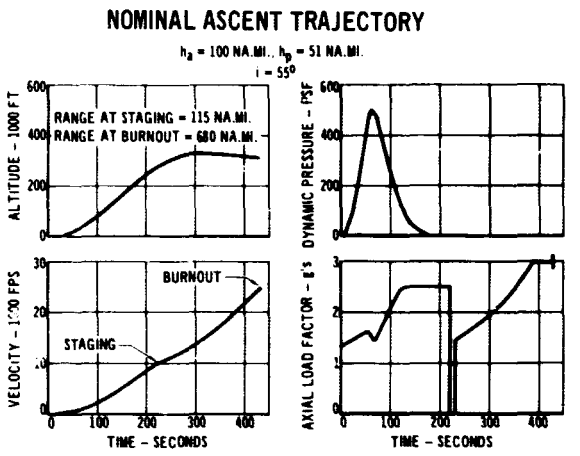

Figure 15

Computer simulations of several possible booster flyback trajectories have been performed to estimate the structural loading and flyback range requirements. The selected control technique involves a negative lift (180° bank angle) during the early low dynamic pressure region to minimize downrange travel. This is followed by a full lift phase to reduce the maximum normal load factor. Following peak load factor, the booster is then banked 80° to turn the velocity vector towards the launch site. A typical trajectory is shown in Figure 16.

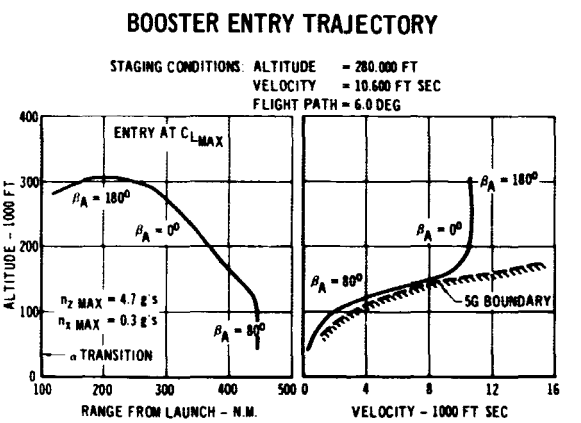

Figure 16

Orbiter entry trajectories were computed from a 55° inclination, 270 NM circular orbit. A nominal entry is shown in Figure 17. The orbiter enters the atmosphere at 60 degrees angle of attack at full lift attitude (zero bank angle). At approximately 260,000 feet, the orbiter begins to pull-out due to the increased aerodynamic lift. The orbiter is then bank modulated at constant angle of attack to maintain a constant altitude until reaching the velocity of a full lift equilibrium guide entry trajectory. The glide entry is then flown until reaching an altitude of approximately 50,000 feet (M = .4) when angle of attack transition is initiated.

The advantage of a 60 degree angle of attack is twofold. First, it is near maximum lift coefficient and therefore yields low entry load factors (1.5 g's) and a low maximum heating rate (62 BUT/ft^2-sec). Secondly, it is a high drag configuration resulting in relative short entry time and low total heat.

The lateral range capability associated with 60 degree angle of attack (L/D = .53) is approximately 230 nautical miles. In combination with the velocity increment available for return phasing (55 ft/sec), 230 nautical miles is sufficient for once a day return capability.

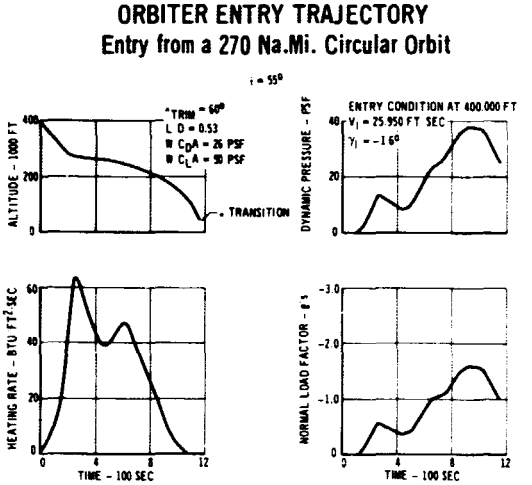

Figure 17

The transition maneuver to bring the angle of attack from 60° during entry to a cruise attitude of about 5° is

shown in Figure 18. After this maneuver the vehicle flys as a conventional aircraft can be flown to a horizontal landing.

ANGLE OF ATTACK TRANSITION TRAJECTORY

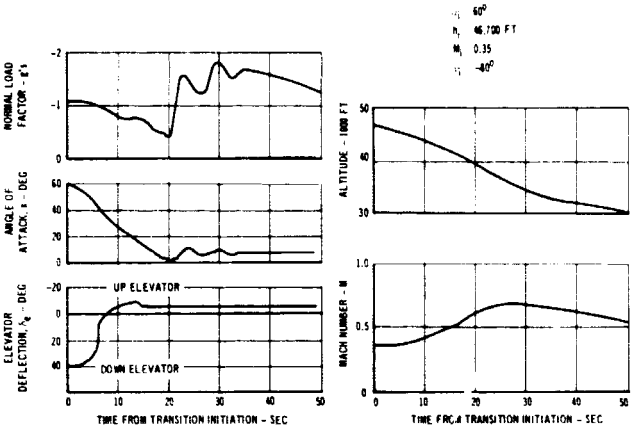

Figure 18

5. Thermal Protection System - A description of the orbiter TPS for entry at 60° is illustrated in Figure 19. Pyrolized carbon laminate is used on the nose cap and wing leading edge regions where temperatures exceed 2500°F. The majority of the upper fuselage surface, upper tail, and upper wing areas are protected with titanium skin because the temperatures are below 800°F. Hardened compacted fiber (HCF) insulation made of silica and bonded to honeycomb sandwich panels is used to protect the lower fuselage area. On the lower wing and tail areas, and on the forward regions of the fuselage, HCF is bonded directly to the titanium skin.

On the bottom and lower side regions of the fuselage a silica HCF material is used with a 15 pcf density. This HCF has a silica cloth facing that is used to provide increased resistance to rain erosion and servicing damage. This facing has a high emittance coating of cobalt oxide. The outer layer of HCF is bonded with a film adhesive to a fiberglass honeycomb sandwich. Adhesive temperatures are limited to 500°F in this design to obtain the maximum reuse capability. The honeycomb sandwich panels are attached to the cryogenic tank rings with titanium structural links. These titanium links are designed to minimize the heat short between the exterior panel and the cryogenic tank rings. A low density fibrous insulation blanket made of TG 15000 is supported across the tops of the cryogenic tank rings to form a prelaunch purge space between the tank wall and the insulation blanket. Holes in the tank rings permit the purge gas flow to pass from one ring section to the next. On the inside of the hydrogen tank a polyurefoam is bonded to the tank wall.

The approach selected for areas on the wing leading edge where the temperatures exceed 2500°F is a replaceable carbon slipper concept. See Figure 10. Inhibited carbon will oxidize where the temperatures exceed 2500°F. After several entry flights this oxidation may change the aerodynamic characteristics of the wing. The replaceable slipper leading edge construction permits a relatively inexpensive part to be designed that can be replaced when necessary. Behind the inhibited carbon slipper is a carbon/carbon honeycomb structure in the leading edge that is good for 100 flights provided the surface of the carbon/carbon never exceeds 2500°F. The slipper consists of a carbon/carbon external surface approximately 3/10 of an inch thick that is backed by zirconia insulation and attached at local spots to the honeycomb sandwich. These attachment points are insulated with zirconia plugs. The slipper is considered only in those areas where temperatures above 2500°F are expected. The actual life prediction for the carbon/carbon slipper leading edge using the worst-on-worst assumptions for the current heating prediction is estimated at 4 flights. If more realistic assumptions are selected in the region of interference heating on the wing leading edge, the slipper design thickness is good for roughly 10 to 30 flights.

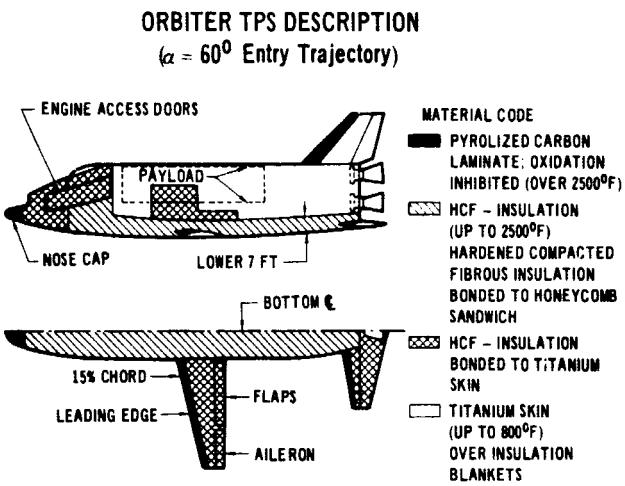

Figure 19

Figure 20 summarizes the total orbiter TPS weight distribution along the fuselage, and the chord-wise weight distribution on the wing. On the bottom centerline, the TPS weight drops sharply on the front 20% of the fuselage length because the HCF is bonded to the titanium skin rather than applied to honeycomb panels. On the wings the TPS weight is slightly heavier at the wing tip (100% of exposed span), because the chord length and the leading edge radius are slightly smaller than at 50% span. The dash line indicates the heavier TPS weight in the inboard region where interference heating is experienced. In all cases the HCF material is bonded directly to wing structure, and the bond line temperature is limited to 500°F. The total TPS weight for the orbiter is 18,450 lbs. This total weight includes HCF, honeycomb panels, structural supports, insulation blankets, base heat protection, and cryogenic foam in the hydrogen tank. The reference fuselage area and wing area protected by TPS are indicated.

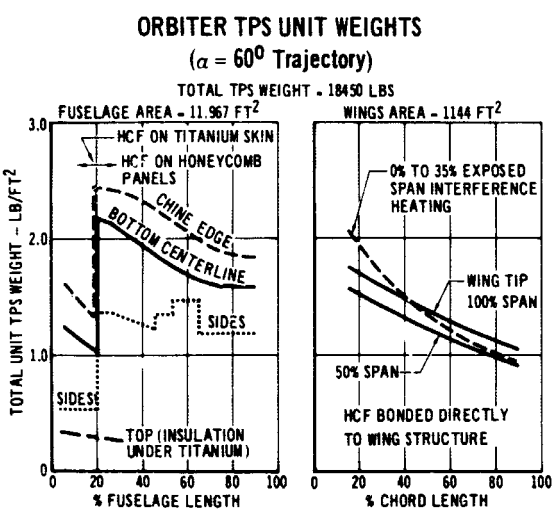

Figure 20

Figure 21 illustrates the booster baseline TPS. The majority of the area is below 800°F and is protected by titanium skin over insulation blankets. Those areas on the lower wing horizontal tail, and the forward areas of the fuselage that exceed 800°F are protected by the hardened compacted fiber insulation. The total TPS weight for the booster is estimated at 30,130 lbs. This weight includes titanium shingles, HCF, insulation blankets, cryogenic foam inside the hydrogen tank, and base heat protection. (Where HCF is bonded directly to titanium that serves as structural skin the titanium is not included in the TPS weight.)

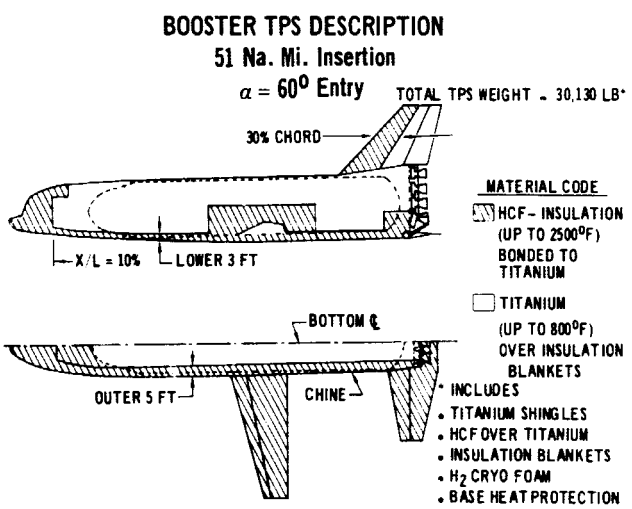

Figure 21

Figure 22 presents the orbiter heating rate distribution along the fuselage bottom and chine region, and the distribution around the circumference of the fuselage. These distributions are for the baseline trajectory (α = 60°) normalized to a fuselage length of 150 ft.

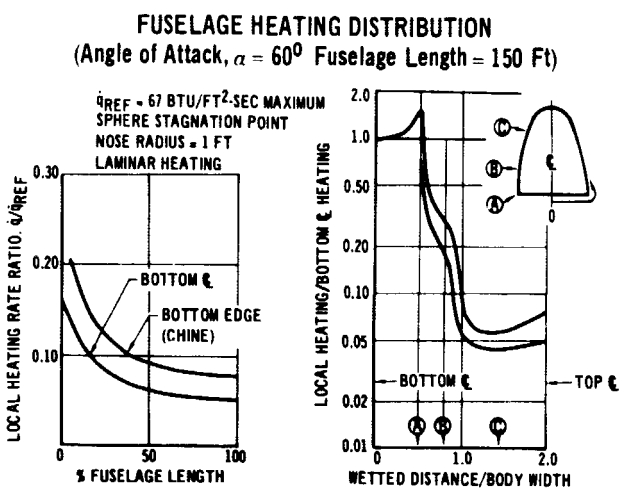

Figure 22

The heating distribution on the wing for the design entry condition is shown in Figure 23. The data shown are from tests conducted by NASA-MSC on a 100% and 40% chord models. The recommended design curve accounting for the flow irregularities and instrumentation difficulties is also indicated.

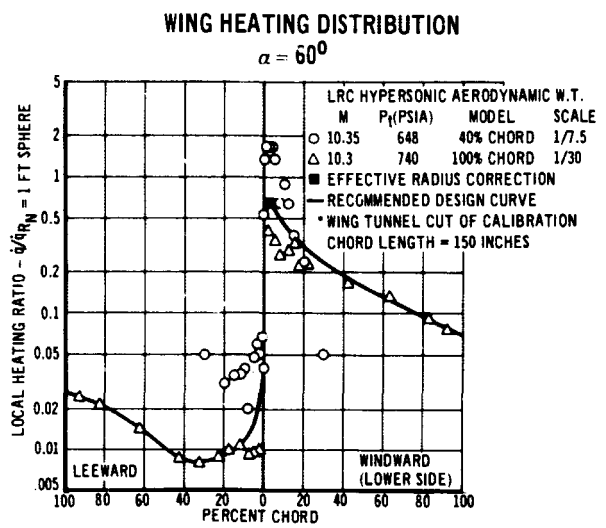

Figure 23

A summary of the data obtained by MSC on wing interference heating is summarized in Figure 24. Two regions are indicated. Region one has two zones and it is thought that this shape is caused by the fuselage bow shock wave combining with the shock wave and flow field around the wing. Region one moves inboard toward the fuselage as the angle of attack is increased. At an angle of attack of 60° the outer edge of the interference region is approximately 35% of the exposed wing span length. Interference region two is caused by boundary layer flow along the fuselage intersecting with the wing. The lower figures show the heating rate increase (or the heating rate multiplier) that is used as a function of chord length for region one and region two at three angles of attack, 15°, 45°, and 60°. Currently there is uncertainty regarding extrapolation of the interference multiplier for the first 15% of chord. However, this is the leading edge region of the wing, where the carbon/carbon replaceable slipper is used which has been sized to endure more than one flight.

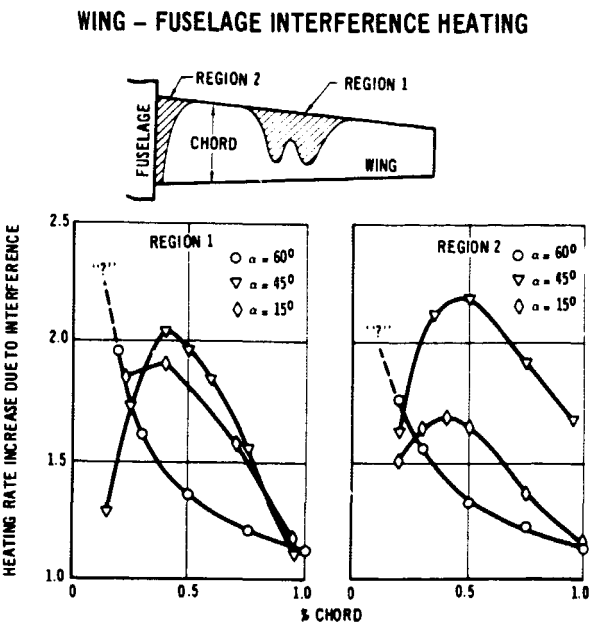

Figure 24

The design trajectories from which the local temperature distribution and the thermal protection system weights were determined is shown in Figure 25.

DESIGN HEATING RATE HISTORIES

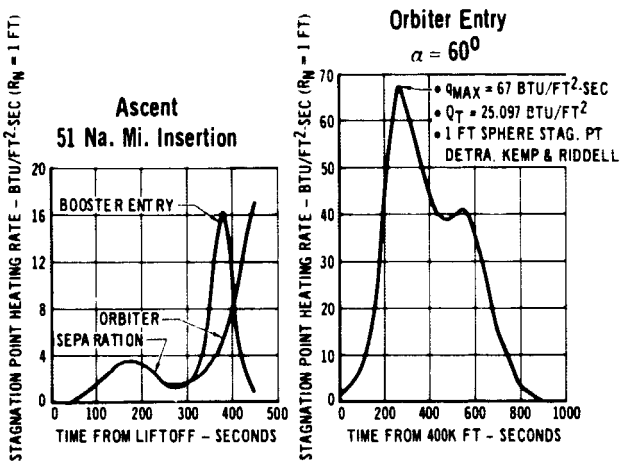

Figure 25

6. Propulsion - The propulsion systems required on the booster and orbiter mission include: (1) a boost propulsion, (2) attitude control, and (3) cruise propulsion for both the booster and orbiter; and an orbit maneuvering system for the orbiter.

The boost engines were sized accounting for the ΔV losses during boost, engine out capability, base area contribution to performance, and commonality of engines between the booster and orbiter. The characteristics selected are summarized as Figure 26. Ten (1) high chamber pressure bell

BOOST ENGINE CHARACTERISTICS

	BOOSTER	ORBITER
TYPE	HIGH P_C BELL	HIGH P_C bell
MIXTURE RATIO	6:1	6:1
AREA RATIO	42.5:1 (FIXED)	100:1 (RETRACTABLE)
WEIGHT	4150	4400
-3σ WEIGHTED IMPULSE PENALTY - SEC	1.6	3.5
NOMINAL THRUST - LB	400,000 (S.L.)	463,000 (VAC)
GIMBAL REQUIREMENTS		
PITCH	±5°	±5°
YAW	±4°	±1°
ROLL	±1°	±1°

Figure 26

nozzle type engines were selected for the booster, and two (2) for the orbiter. All boost engines are throttleable. The engines are designed for 100 mission life with a 10 hour life between overhaul.

Figure 27 shows the boost engine feed system geometry. Five 14" dia. lines run from the oxidizer tank with each line splitting into two 10" dia. lines. The line division is positioned such that a vapor bubble generated by an engine shut down will not be ingested by another engine. Engine isolation valves are located immediately downstream of the line division. The ten resulting lines are then routed to each boost engine as shown. Diffusers are used to transition smoothly from the 10" dia. lines to the required 14" dia. engine supply. Pressure/volume compensators and gimbal bellows assemblies are used immediately upstream of the engines. The oxidizer tank incorporates anti-vortex and slosh baffles.

BOOST ENGINE FEED SYSTEM

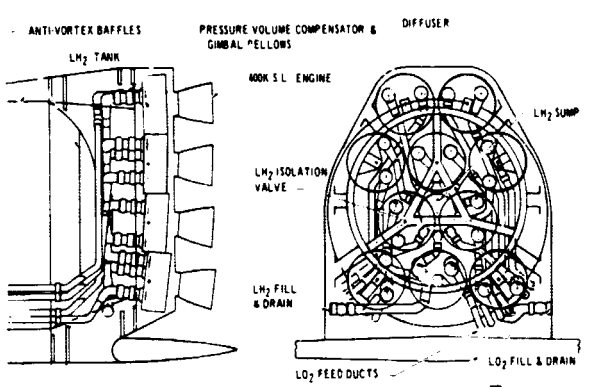

Figure 27

The hydrogen feed system is generally similar, except that due to the relative close coupling of the hydrogen tank and the engines, the hydrogen lines are initially fed from a compartmented sump. Engine shut-off valves are located at the sump outlets. The hydrogen tank also incorporates a multicruciform anti-vortex baffle assembly

and slosh baffles. The compartmented sump and the anti-vortex tank baffle are configured so that any vapor bubble generated by an engine shut-down can not be ingested by another engine. Single point fill/drain vehicle/AGE interfaces are used for each propellant. Initial helium engine requirements are ground supplied. Upon engine start-up, bleed GH_2 and bleed GOX are used to pressurize the hydrogen and oxygen tanks respectively. The boost feed system for the orbiter is similar and is schematically shown by Figure 28.

NOMINAL ΔV BUDGET

	OMS	RCS
NOMINAL MISSION FUNCTIONS		
ORBIT TRANSFER AND CIRCULARIZATION	660 FT SEC	
TERMINAL RENDEZVOUS		60 FT SEC
DOCKING AND STATIONKEEPING		30 FT SEC
DEORBIT (INCL 10% RESERVE)	535 FT SEC	
DISPERSIONS		
PRECEEDING TERMINAL RENDEZVOUS		120 FT SEC
DURING TERMINAL RENDEZVOUS		90 FT SEC
GROUND TRACK ADJUSTMENTS		55 FT SEC
VELOCITY INCREMENT REQUIRED	1195 FT SEC	355 FT SEC
VELOCITY MARGIN	450 FT SEC	
TOTAL VELOCITY PROVIDED	2000 FT SEC	

Figure 29

ORBITER BOOST ENGINE FEED SYSTEM

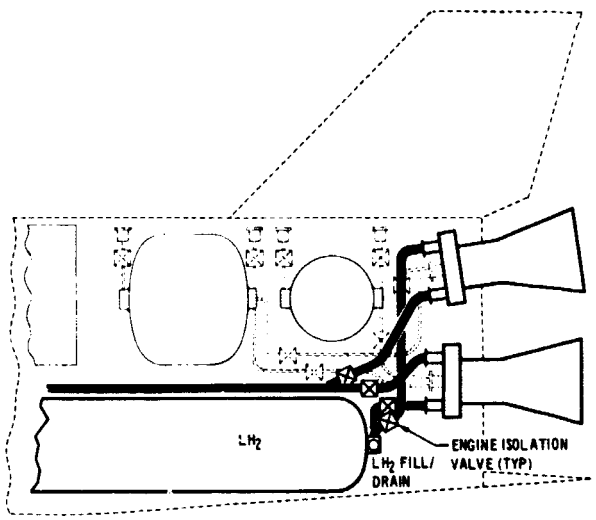

Figure 28

RCS REQUIREMENTS

FUNCTION	ΔV - FT SEC	THRUST WT	α - DEG SEC²			TOTAL IMPULSE (LB-SEC)	PROPELLANT REQUIRED LB (1)
			PITCH	ROLL	YAW		
ORBITER							
TERMINAL RENDEZVOUS	60	0.016 (FORE AFT) 0.004 (OTHER)	-	-	-	405,000	1310
DOCKING	30		0.5	0.5	0.5	203,000	655
ORBIT ACS	-	-	-	-	-	326,000	1050
ROLL DISTURBANCE (BOOST ENGINE OUT)	-	-	-	50 (4)	-	-	(3)
DISPERSIONS	265	-	-	-	-	1,775,000	5730
RE-ENTRY	-	-	SMALL	1.0	1.73	360,000	1160
BOOSTER							
SEPARATION (2)							
RE-ENTRY (2)						776,000	2500

(1) BASED ON I_{VAC} 310 SEC, 1.5
(2) REQUIREMENTS NOT DEFINED - ORBITER ARRANGEMENT WILL BE USED PENDING FURTHER DEFINITION
(3) PROPELLANT DRAWN FROM ORBIT RCS BUDGET
(4) EQUIVALENT TO 60,000 FT-LB ROLL TORQUE AT 1.2 DEG YAW GIMBAL

Figure 30

On-orbit maneuvering and attitude control requirements are dictated by the nominal ΔV budget (Figure 29) and the required translational and angular acceleration response characteristics (Figure 30). The initial circularization, orbit transfer and retro are performed by the orbit maneuvering system. Gross attitude control during these burns is provided by gimballing the engines. All other orbital and reentry translational and attitude maneuvers are performed by the RCS.

The large orbital maneuvers may be satisfied by using one or both of the orbiter boost engines at reduced thrust level, or by adding an additional engine system, e.g. two additional RL-10 engines. A trade study comparing the weight of possible alternatives was made. The lightest maneuver system is obtained with either the use of an advanced design high Pc bell nozzle engine operating in a pressure fed mode at 1% thrust, or the use of two additional RL-10 engines. The advanced design pressure fed concept has been based on the performance potentially achievable if an engine design could be developed for optimum performance at both 100% and 1% thrust levels. The current design high Pc engine performance is

estimated to be approximately 30 seconds lower in Isp, which causes the pressure fed system to be 2000 pounds heavier than the RL-10 installation. Since the advanced design pressure fed and the RL-10 concepts are essentially equal in weight, the pressure fed concept was selected for the baseline design to avoid the installation of additional engines. Figure 31 schematically shows the general arrangement of the pressure fed mode orbit maneuvering system. Note that the propellant is drawn from separate cryogenic storage tanks located in the aft section of the orbiter.

ORBIT MANEUVER FEED SYSTEM

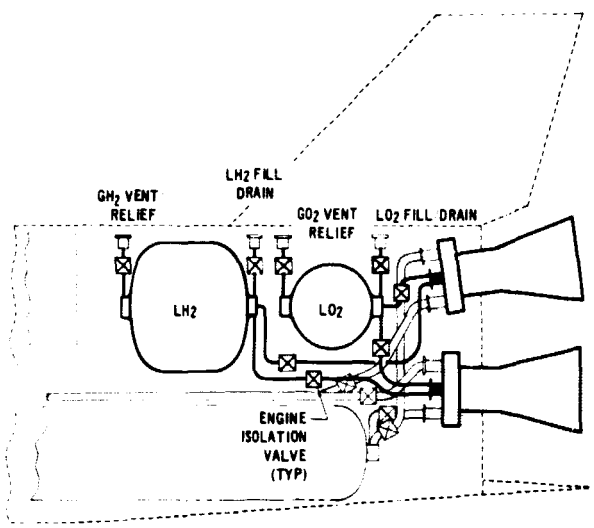

Figure 31

The number of RCS engines and the engine thrust levels may, for attitude control, be held to a minimum by utilizing a combination of wing mounted and fuselage mounted engines as shown in Figure 32. The translation engines are also used for pitch and yaw attitude control, with roll control provided by additional wing mounted engines. Arrangements without wing mounting were considered but would require additional engines or higher thrust levels to satisfy the yaw and roll requirements.

RCS ENGINE ARRANGEMENT

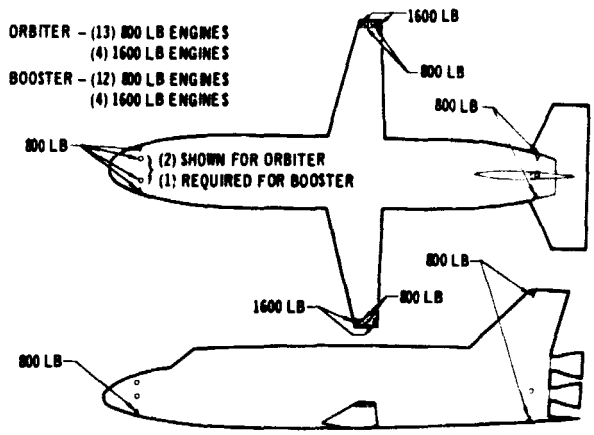

Figure 32

A subsonic cruise propulsion subsystem is incorporated on both the booster and the orbiter to provide the capability of (1) cruise back to the landing site (booster only) and/or landing assistance (booster and orbiter), (2) go-around at the landing site, and (3) cross-country ferrying. The cruise propulsion performance requirements for each of these operations are summarized in Figure 33. In addition, the study requirements were that only off-the-shelf engines using conventional JP fuel were to be considered in detail.

CRUISE PROPULSION REQUIREMENTS

- CRUISE
  - BOOSTER
    - RETURN TO LAUNCH SITE
    - RANGE CONTINGENCY - 20%
    - ENGINE-OUT - MAINTAIN 4000 FT MINIMUM ALTITUDE
  - ORBITER
    - NO CRUISE REQUIREMENT
- LANDING
  - BOOSTER AND ORBITER
    - TOUCH-DOWN VELOCITY - LESS THAN 140 KNOTS
    - ROLL-OUT - CONSISTENT WITH 8000 FT RUNWAY
- GO-AROUND
  - BOOSTER AND ORBITER
    - CLIMB RATE - GREATER THAN 2000 FT/MIN AT S.L.
    - PROPELLANT REQUIREMENT - 5 MIN AT TAKE-OFF POWER
    - ENGINE-OUT - GO-AROUND NOT REQUIRED
- FERRY
  - BOOSTER AND ORBITER
    - CLIMB RATE - GREATER THAN 400 FT/MIN AT S.L.
    - RANGE - GREATER THAN 400 MILES
    - AUXILIARY PROPULSION AND TANKAGE PERMISSIBLE
    - NO PAYLOAD
    - ENGINE-OUT - MAINTAIN 4000 FT MINIMUM ALTITUDE

Figure 33

The baseline orbiter cruise propulsion installation can be seen in Figure 4. In this configuration four (4) JT8D-9 turbofan engines are mounted within the forward fuselage. The JP fuel is stowed in wing tankage. Doors are installed in each of the four engines inlet ducts to protect the engines from boost and entry heating. The engine duct losses were estimated to be 5%.

The engine exhaust ducts are canted 20° to the vehicle axis. The cosine losses were considered but exhaust scrubbing losses on the side of the vehicle were not evaluated. A detailed study of the effective thrust loss and the effects of noise and vibration induced on the sides of the orbiter should be accomplished in future studies.

Unlike the orbiter, the booster has a long range cruise back requirement. For this reason a significant portion of the system weight is fuel and the operating duration of the engine will be hours instead of minutes. Thus the engine selection for the booster should have the characteristics of low specific fuel consumption rate and significant operating life. The baseline configuration uses six (6) JT3D-7 turbofan engines mounted in the forward fuselage as shown in Figure 6.

7. Integrated Avionics - The basic rationale for the use of Integrated Avionics is derived from the measures required to achieve economy of operation. These measures are a self contained, crew controlled, prelaunch checkout capability, rapid turn around/reuse capability and a higher degree of mission success. Avionic capabilities must include self checkout, block and functional redundancy, and maintenance to a Line Replaceable Unit (LRU). To ensure compatibility with manned control, the Integrated Avionics system will provide a highly efficient data management and display/control capability. It will relieve the crew of excessive workload by automatically performing time critical functions and by providing priority sorting and data compression of that information needed by the crew.

The general avionic functions are:

- o Vehicle Self Test and Warning
- o Data Processing and Transfer
- o Crew Command and Integrated Displays
- o Target Tracking
- o Autonomous Navigation and Flight Control
- o Satellite Communications
- o Supporting Energy Conditioning

The key questions to be answered in order to define the Integrated Avionics System are: the means of implementing Data Management; On-Board Checkout; Display and Control; and Reliability, as well as, Reuse. The features that were evaluated in preliminary tradeoffs in this study are indicated in Figure 34.

KEY QUESTIONS

DATA MANAGEMENT	• COMPUTATIONS - DECENTRALIZED • INTERFACE TECHNIQUE (MULTIPLEXED)
ONBOARD CHECKOUT	• BUILT IN TEST • LEVEL OF FAULT ISOLATION AND MAINTENANCE
DISPLAY AND CONTROL	• MULTIMODE INTEGRATED DISPLAYS • AUTOMATIC SEQUENCING
RELIABILITY & REUSE	• REDUNDANCY AND SELF TEST • MALFUNCTION DETECTION AND SWITCHOVER • MAINTENANCE PHILOSOPHY

Figure 34

The elements of the Integrated Avionics system are shown in Figure 35. Equipment and configuration selection was made on the basis of: (1) an estimate of the 1972 technology status and, (2) use of concepts which provide small development risks.

BASELINE ORBITER INTEGRATED AVIONICS SYSTEM

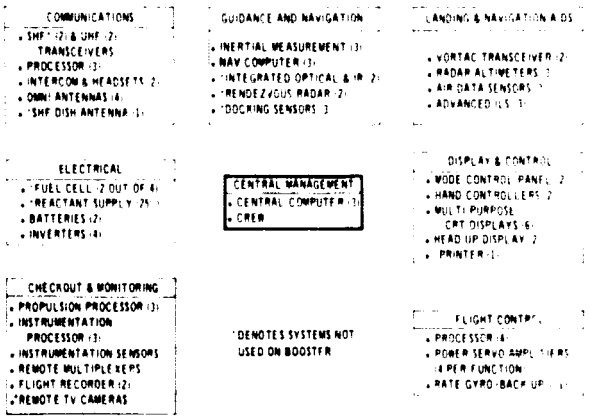

Figure 35

DISPLAY ARRANGEMENTS

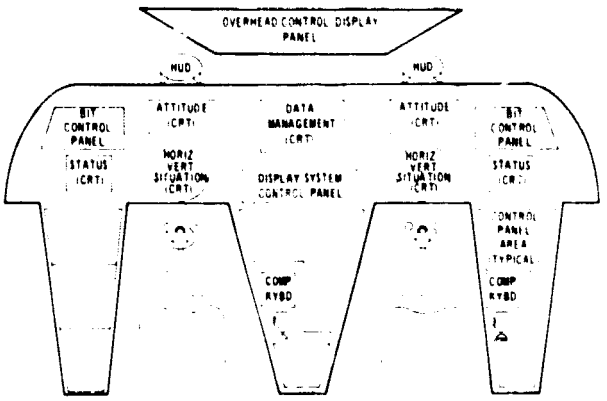

Figure 36

Inertial sensors are used as the prime source of navigation data through all active mission phases. Choice of inertial systems in both the booster and orbiter were dictated by the ascent guidance, entry to a pre-determined landing site and automatic landing requirements. Star trackers and horizon sensors provide autonomous on-orbit attitude and navigational updates. The multi-mode rendezvous radar provides for rendezvous with either cooperative or non-cooperative vehicles. A dedicated navigation comptuer supplies the unique requirements of individual system sensors while permitting the central software programming tasks to be maintained at a manageable complexity level. This keeps sensor unique computational requirements from impacting the central computational requirements.

The UHF communication link is utilized for EVA, inter-vehicle voice or data, and airport communication during the approach and landing phase. The Comsat-link provides nearly continuous communication capability between any ground station and the orbiter during the orbital phase of flight.

The display concept utilizing cathode ray tubes for multimode data presentation permits crew decisions on important tasks while relieving them of the need to monitor a large number of displays and meters. A typical cockpit display arrangement is shown in Figure 36.

A common, multiplexed data bus was selected to provide standardized digital interfaces, and to reduce the complexity and weight of interconnecting systems. The intermix of computers consists of a central data processor to perform mission oriented functions, and peripheral dedicated computers for sensor functions, navigation, flight control, and propulsion computations. This arrangement was chosen on the basis of commonality of requirements while maintaining equipment and software at manageable complexity levels. Thus, sensor oriented computational requirements, both hardware and software, do not impact the central computer.

On-board checkout minimizes ground support and expedites maintenance and reuse. Decentralized Built-In Test (BIT) was selected over a separate centralized test system to minimize interface complexity and provides subsystem functional automomy. BIT provides self-test at all maintenance levels and permits identification of failures to the line replaceable units. Selective computer controlled areas for flight, caution and warning, or ground base checkout.

Figure 37 shows size, power, and weight of the selected equipment. Booster equipment is identical to that of the orbiter except that equipment utilized only for orbital operations is deleted. Such equipment, as well as, the level of equipment redundancy, is identified in Figure 35.

ORBITER INTEGRATED AVIONICS
PHYSICAL CHARACTERISTICS

EQUIPMENT TYPE	WEIGHT (LB)	SIZE (CU FT)	OPERATING POWER (WATTS)
GUIDANCE & NAVIGATION	720	11.8	2270
LANDING & NAVIGATION AIDS	170	3.05	460
COMMUNICATIONS	325	48.85	545
CENTRAL MANAGEMENT COMPUTER	180	3.0	500
DISPLAYS & CONTROL	477	8.25	1525
FLIGHT CONTROL	197	3.55	1115
CHECKOUT & MONITORING	125	2.1	260
ELECTRICAL	1860	37.0	10 KW (CAPACITY)
PWR DISTR AND CONTROL WIRE	700	10.0	
SIGNAL DISTR WIRE	1300	20.0	
TOTAL ORBITER AVIONICS	6054	147.6	5765 (PEAK)
TOTAL BOOSTER AVIONICS	3900	60.0	5042 (PEAK)

Figure 37

8. Technology and Development Plan - This development test program provides a basis for establishing development costs, schedules, and identification of time critical development effort where additional definition and study is required. A summary schedule illustrated in Figure 38 is based on parallel development of the Orbiter and the Booster and assumes that technology and research funding is adequate to demonstrate feasibility of all technologies prior to go-ahead on Phase D. The development, manufacturing and flight tests efforts of this schedule are considered to be the minimum allowable. The operational program was assumed to have one launch per month and require three orbital vehicles and two boosters to meet this schedule. Initial Operation Capability (IOC) occurs in mid-July 1976 and all five production vehicles are utilized for flight testing.

SUMMARY DEVELOPMENT SCHEDULE

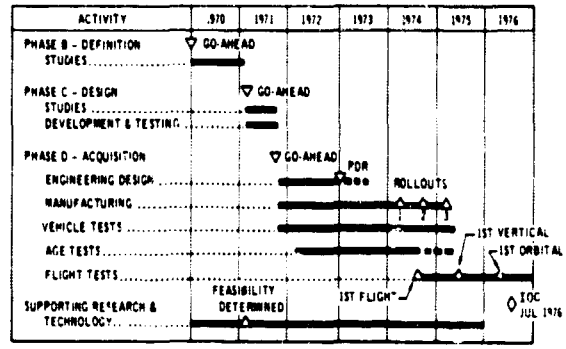

Figure 38